



NIH PUBLIC ACCESS

Author Manuscript

Cancer Res. Author manuscript; available in PMC 2011 November 1.

Published in final edited form as:

Cancer Res. 2010 November 1; 70(21): 8435–8445. doi:10.1158/0008-5472.CAN-10-1506.

K-ras mutation targeted to gastric tissue progenitor cells results in chronic inflammation, an altered microenvironment, and progression to intraepithelial neoplasia

Tomoyuki Okumura^{1,*}, Russell E. Ericksen^{1,*}, Shigeo Takaishi¹, Sophie S.W. Wang¹, Zinaida Dubeikovskiy¹, Wataru Shibata¹, Kelly S. Betz¹, Sureshkuma Muthupalani², Arlin B. Rogers³, James G Fox², Anil K Rustgi⁴, and Timothy C Wang¹

¹Division of Digestive and Liver Diseases, Columbia University Medical School

²Division of Comparative Medicine, Massachusetts Institute of Technology

³Lineberger Comprehensive Cancer Center, University of North Carolina at Chapel Hill

⁴Departments of Medicine and Genetics, University of Pennsylvania Medical School

Abstract

Chronic infectious diseases, such as *Helicobacter pylori*, can promote cancer in a large part through induction of chronic inflammation. Oncogenic K-Ras mutation in epithelial cells activates inflammatory pathways, which could compensate for a lack of infectious stimulus. Gastric histopathology and putative progenitor markers (Dcamk11, Keratin 19) in Keratin 19-K-Ras-V12 (K19-kras) transgenic mice were assessed at 3, 6, 12 and 18 months of age, in comparison with *Helicobacter felis* (*H. felis*)-infected wild-type littermates. Inflammation was evaluated by RT-PCR of pro-inflammatory cytokines, and K19-kras mice were transplanted with GFP-labeled bone marrow. Both *H. felis* infection and kras mutation induced upregulation of pro-inflammatory cytokines, expansion of Dcamk11⁺ cells, and progression to oxyntic atrophy, metaplasia, hyperplasia and high-grade dysplasia. K19-kras transgenic mice uniquely displayed mucous metaplasia as early as 3 months, and progressed to high-grade dysplasia and invasive intramucosal carcinoma by 20 months. In bone marrow transplanted K19-kras mice that progressed to dysplasia, a large proportion of stromal cells were GFP⁺ and bone marrow-derived, but only rare GFP⁺ epithelial cells were observed. GFP⁺ BMDCs included leukocytes and CD45⁻ stromal cells that expressed vimentin or α SMA and were often found surrounding clusters of Dcamk11⁺ cells at the base of gastric glands. In conclusions, the expression of mutant Kras in K19⁺ gastric epithelial cells can induce chronic inflammation and promote the development of dysplasia.

Correspondence information: Timothy C Wang, 1130 St. Nicholas Avenue, Room 925, Columbia University Medical Center, New York, NY 10032, Phone: (212) 851-4581, Fax: (212) 851-4590, tcw21@columbia.edu.

Authors' contribution:

Tomoyuki Okumura: Conception and design, experiment, manuscript writing.

Russell Ericksen: Conception, experiment, manuscript writing.

Shigeo Takaishi: Conception, experiment.

Sophie Wang: Conception, experiment.

Zinaida Dubeikovskiy: Conception, provision of study materials

Wataru Shibata: Conception, experiment

Kelly Betz: Conception, experiment

Arlin B Rogers: Pathological diagnosis

James G Fox: Pathological diagnosis

Anil Rustgi: Conception, provision of study materials.

Timothy Wang: Conception and design, manuscript writing.

*These two authors equally contributed for this study.

Keywords

Bone marrow derived cells; Gastric epithelial stem cells; Gastric cancer; Kras mutation

Introduction

Helicobacter-related gastric cancer arises through a multistage progression that involves the conversion of normal gastric epithelium to regions of hyperplasia, dysplasia and finally, invasive adenocarcinoma. This multistep process is associated with the accumulation of genetic and/or epigenetic alterations in the target cell population that leads to their malignant transformation. *Helicobacter* infection contributes to the pathogenesis of gastric cancer in a large part through the induction of chronic inflammation (1,2), which can induce proliferation and thus opportunity for mitotic error. In addition, *Helicobacter* infection can promote the development of cancer through mobilization and recruitment of bone marrow-derived cells (BMDCs) that contribute to cancer development in diverse ways (3-5).

However, while chronic inflammation can likely initiate and promote oncogenic mutation and transformation, accumulating data suggests that in many cases the converse is also true, and that oncogenic mutations can also lead to the development of chronic inflammation (6). Cytokines and soluble mediators produced by oncogene mutations in cancer cells recruit and activate inflammatory cells to develop a tumor microenvironment, which further stimulate tumor progression (6,7).

One oncogene that has been strongly linked to the development of chronic inflammation has been the Ras oncogene (8). Expression of a mutant K-ras oncogene induces strong immune responses through activation of cytokines and T cells (9-11). In transgenic mice modeling pancreatic cancer, based in part on K-ras mutations in PDX1⁺ cells, significant inflammatory and stromal responses correlate with cancer progression (12). Expression of the mutant K-ras-V12 oncogene in cyokeratin-19 (K19)-expressing pancreatic cells also results in pancreatic ductal hyperplasia with lymphocytic infiltration (13). Studies from *Bar-Sagi et al.* showed that many of the key downstream targets of K-ras were chemokines and cytokines (10,14). Further studies demonstrated that transformed cell survival and tumor progression are dependent on these induced cytokines (15).

In a previous report, K-ras-V12 was expressed in the gastric epithelium using the K19 promoter, and resulted in mucous metaplasia and parietal cell loss (13). However, a detailed investigation the inflammatory responses and development of dysplasia in this model has not yet been reported. K19 is a member of the family of intermediate filaments that is highly expressed in the proliferative zone of the gastrointestinal tract (13,16-18). In the stomach, K19 is expressed in the neck/isthmus region of the glandular unit, in the same area where stem/progenitor cells reside (13,16). In theory, induction of cancer is most likely to occur when oncogenic mutations accumulate in long-lived stem or progenitor cells. While an authentic stem or progenitor cell for the oxyntic glands of the stomach as not yet been identified, one candidate progenitor marker that has emerged is Doublecortin and calcium/calmodulin-dependent protein kinase-like-1 (Dcamk1), a gene shown to be upregulated in an enriched gastric epithelial progenitor cell population from the murine fundus (19). Dcamk1⁺ cells reside in the neck/isthmus region of the stomach glands and do not express biomarkers associated with differentiated lineages (19,20).

The aim of the current study was to compare the effects of mutant K-ras expression to chronic *H. felis* infection on the gastric epithelium. We show that mutant K-ras can substitute for

Helicobacter infection in the induction of chronic inflammation, leading to expansion of putative gastric progenitors and induction of gastric intraepithelial neoplasia (GIN).

Materials and Methods

Mice

The K19-K-ras-V12 (K19-kras) transgenic mice were generated previously (13), using a 2.1-kb genomic fragment of the 5 flanking region/promoter of the mouse K19 gene linked to the full-length mutant human K-ras (Val 12) gene. K19-K-ras-V12 transgenic mice were backcrossed to C57/BL6 mice for at least 3 generations under the Columbia University IACUC. Chicken beta-actin EGFP transgenic mice (8-10 weeks old) were purchased from Jackson Laboratories (Bar Harbor, ME).

H. felis infection, histopathology and immunocytochemistry

H. felis infection was carried out by gavage as previously described with *H. felis* (ATCC 49179) (4). Stomachs were fixed in 10% neutral buffered formaldehyde and routine hematoxylin and eosin (H&E) sections were reviewed by board-certified veterinary pathologists and graded according to previously described criteria (21,22). Immunohistochemistry was performed on 4 μ m sections with avidin biotin-peroxidase complex kits (Vector Laboratories, Burlingame, CA) and counterstained with Mayer's hematoxylin. For primary antibodies, mouse anti-Hydrogen/Potassium ATPase (H/K-ATPase) beta (Affinity BioReagents, Golden, CO), rabbit anti-Ki67 (Abcam), rabbit anti-Cytokeratin 19 (Abcam), rabbit anti-Dcamk11 (Abagent), rabbit anti-mouse-TFF2 (established in our laboratory), rabbit anti-TFF1 (Abcam) and mouse anti-Muc5AC (Abcam) or rabbit anti-GFP (Invitrogen) were used.

PCR and qRT-PCR analysis

Real-time PCR reactions with QuantiTect SYBR green PCR kit (QIAGEN, Maryland, MA) and primers (Suppl. Table 1) were run on an ABI Prism 7300 (Applied Biosystems, Branchburg, NJ). mRNA quantities were analyzed in duplicate and normalized against GAPDH as an internal control. Results are expressed as relative gene expression using the $\Delta\Delta$ Ct method.

Bone marrow transplantation

Bone marrow transplantation was carried out as previously described with 5 million cells/animal (3). Mice were euthanized at 3, 6, and 12 months post-transplantation.

Flow cytometry and MSC culture

Freshly isolated bone marrow cells were processed for flow as previously described (4,6) and after incubation with PE-conjugated anti mouse CD45 antibody (BD Pharmingen, San Diego, CA) or PE-conjugated rat IgG2a antibody (isotype control) Jackson ImmunoResearch, West Grove, PA) and DAPI, were analyzed using BD LSR II (Becton, Dickinson). Mesenchymal stem cells were cultured as previously described (23).

Y chromosome and Keratin 19 *in situ* hybridization

In situ hybridization for Y-chromosome or K19 were performed using a Texas Red-labeled Y-chromosome paint (Star-FISH; Cambio, Cambridge, UK) or a DIG-labeled antisense riboprobe (Roche) following manufacturer's protocols, as previously described (24).

Immunofluorescence

Immunofluorescence was performed following in vitro fixation-perfusion with 4% paraformaldehyde followed by freezing and embedding in OCT and frozen. 4 μ m sections were prepared and blocked with 1% FBS in PBS for 1 hour at room temperature, then rat anti-E-cadherin antibody (Zymed, South San Francisco, CA), rat anti-CD45 (eBioscience), rabbit anti- α SMA (Abcam), rabbit anti-cytokeratin 19 (Abcam), rabbit anti-Dcamk11 (Abagent), mouse anti-vimentin (Abcam), diluted in PBS with 1% FBS (1:100 dilution) were applied. Following overnight incubation at 4°C, Texas Red conjugated anti-rat, rabbit or mouse IgG antibodies (Jackson ImmunoResearch) were applied, respectively, with 1% FBS in PBS (1: 300 dilution) and incubated for 1 hour at room temperature. Nuclei were stained with DAPI, and mounted using Vectashield (Vector Laboratories) for microscopy.

Statistical Analysis

Statistical analysis was performed using t test and p values <0.05 were considered significant. Data are expressed as mean \pm SEM.

Results

K19-kras mice developed gastric hyperplasia and histologic inflammation

To assess the effects that the 2.1kb K19 promoter-driven mutant K-ras-V12 oncogene has on the induction of chronic inflammation, we first investigated the gross appearance, gastric histopathology, and inflammatory responses in K19-kras transgenic mice in comparison to *H. felis*-infected wild type (WT) mice over time. Colonization of *H. felis* in pyloric and fundic glands of WT mice was confirmed by examination of H&E-stained sections and PCR amplification of *H. felis*-specific DNA sequence (Figure S1). Wet stomach weight and the ratio of wet stomach weight to body weight of K19-kras mice were significantly higher than those of control mice, regardless of *H. felis* infection (Figure 1A). This was consistent with the gross appearance of the stomach, where severe mucosal thickness and enlarged folds was consistently observed in K19-kras mice (Figure 1B).

Histopathologic scoring of H&E-stained gastric tissue sections from mice in each group using previously published criteria (21,22) showed that *H. felis*-infected WT mice exhibited much greater chronic active gastritis, oxyntic atrophy, intestinal metaplasia, hyperplasia, and dysplasia that progressed over time (Figure 1C), consistent with the multistage model of *Helicobacter*-related gastric carcinogenesis (22). Inflammation scores in K19-kras mice were similar to that of WT mice with *H. felis* infection. K19-kras mice also developed oxyntic atrophy, pseudopyloric metaplasia, hyperplasia, and dysplasia by 3 months, and the lesions persisted until the end of the study (Figure 1D). Mucous metaplasia, characterized by replacement of parietal cells with foamy Alcian blue-staining H/K-ATPase⁻ cells without glandular dysplasia, was observed in the oxyntic mucosa of K19-Kras mice, but not in wild type mice, even with *H. felis* infection (Figure 1C), consistent with previous reports (13,22). The K19-kras mice also showed a marked lymphocytic infiltrate with hyperplastic lymphoid follicles, similar in appearance and frequency to those found in *H. felis*-infected WT mice (Figure S2A). These results demonstrate that K-ras mutation in epithelial cells is sufficient to induce chronic inflammatory responses in the gastric epithelium.

Oncogenic K-ras mutation in gastric epithelial cells upregulates cytokine and chemokine expression

The finding of chronic inflammation in K19-kras mice suggested that K-ras mutation in gastric epithelial cells triggered the activation of specific immune responses that may be similar to *H. felis*-related chronic gastritis. RT-PCR analysis of mice 6-12 months of age revealed increased

gastric mRNA expression of IL-6 and IL-1 β in both *H. felis* infected WT and K19-*kras* mice, compared to WT uninfected controls (Figure 2A). Additionally, CXCL1 was upregulated in both these groups, while the expression of CXCL5 was up regulated only in K19-*kras* mice (Figure 2B). Interestingly, CXCL1 and IL-6 expression retained the highest degree of correlation with dysplasia scores in K19-*kras* mice (Figure 2C). Similar trends were observed for IL-1 β and CXCL5, albeit with smaller R² values. There were no differences among the three cohorts in the expression of other detected cytokines and chemokines, including IFN γ , TNF α , CCL2, CCL3, and CXCL2 (data not shown). In younger (3 month) mice, expansion of pit cells was moderate (Figure S2B). Consequently, at this point, the aforementioned inflammatory cytokines were minimally elevated, while the chemokine CXCL1 was significantly upregulated (Figure S2B), supporting an important role for CXCL1 in phenotype development. Although *Kras* is known to induce COX-2 expression which can drive tumorigenesis (25), we were unable to detect any upregulation of COX-2 expression in younger mice (\leq 12 months); in contrast, expression was nearly 3-fold higher in K19*kras* over WT mice over 12 months of age, correlating with progression to dysplasia (Figure S3).

Expression of growth factors HB-EGF and amphiregulin was significantly upregulated in the stomachs of K19-*kras* mice when compared to WT mice, regardless of *H. felis* infection (Figure 2D). These results suggest that progression of gastric pre-neoplastic lesions in K19-*kras* mice occurs in the setting an inflammatory environment similar to that found in *H. felis*-dependent chronic gastritis, characterized by expression of CXCL1, IL-1 β , and IL-6. However, the unique phenotype of the K19-*kras* mouse is associated with expression of additional inflammatory chemokines and growth factors that are relatively specific to the K-ras-V12 mutation, which include CXCL5, HB-EGF, and amphiregulin.

Dcamk11⁺ putative tissue stem/progenitor cells are expanded in the preneoplastic gastric lesions of K19-*kras* mice

The progression to metaplasia and dysplasia in the stomachs of K19-*kras* mice was associated with changes in epithelial differentiation and proliferation. In the stomach of normal WT mice, K19 staining was observed primarily in pit cells which comprised the upper one sixth of the gastric glands (Figure 3A). Ki67⁺ proliferating cells reside in the isthmus and upper neck region (Figure 3C), in close proximity to rare Dcamk11⁺ cells found in this region (Figure 3D). Throughout and below the neck region are H/K-ATPase⁺ parietal cells, which make up the majority of glands (Figure 3B).

The gastric epithelium of K19-*kras* mice at 12 months of age displayed obvious parietal cells loss, with only a small number of H/K-ATPase⁺ cells remaining at the base of the gastric glands (Figure 3F). Excluding these rare parietal cells, a majority of the remaining cells were mucus-producing K19⁺ pit cells (Figure 3E), which had expanded to comprise nearly 2/3^{rds} of the entire gland, consistent with previous reports (13). Expression of TFF1 and Muc5AC in the K19-*Kras* mouse stomach indicated that the majority of K19⁺ cells in the upper middle region of glands were expanded surface pit cells (Figure S4A,B). Ki67⁺ proliferating cells shifted over time from the neck region to the bottom of gastric glands, slightly above the remaining parietal cells. Interestingly, the number of Dcamk11⁺ cells increased markedly to many cells in each glandular unit, located just below the proliferative zone and just above the residual parietal cells (Figure 3G, H). It should be noted that Dcamk11 is strictly a putative progenitor marker based on its homeostatic location and frequency throughout the gastric epithelium. *Lgr5* can give rise to gastric antral glands in the murine adult, but *Lgr5* is not expressed in the adult gastric corpus (26). We confirmed that *Lgr5*-EGFP is expressed at the base of gastric antral glands, while Dcamk11⁺ cells reside slightly above, never co-localizing (Figure S4C). Therefore, these results suggest that the Dcamk11⁺ putative epithelial progenitor pool expands

independent of Lgr5 expression, under inflammatory responses induced by mutant K-ras expression.

K19-K-ras-V12 mice develop high grade dysplasia by 20 months of age

We followed a cohort of aged mice, combining data from mice that survived 16 to 21 months of age, to investigate possible progression of the gastric preneoplastic lesions. As expected, K19-kras mice and *H. felis*-infected WT mice continued to exhibit higher inflammation scores when compared to WT mice without *H. felis* infection, becoming progressively more severe with longer observation periods (Figure S5, **see also** Figure 1D). Histology scores for dysplasia were also elevated after long-term observation, in parallel with the severity of inflammation (Figure 4A, **see also** Figure 1D). Among these mice, 3 of 4 (75.0%) *H. felis*-infected wild type mice and 3 of 8 (37.5%) K19-kras mice developed gross papillary tumors in the stomach (Figure 4B). The lesions of three K19-kras mice were histologically defined as high-grade dysplasia or intramucosal carcinoma, with some areas invading into sub-mucosal layers (Figure 4C).

Immunohistochemistry on serial tissue sections revealed that the lower portions of dysplastic glands contained a mixture of TFF2⁺ and Dcamk11⁺ cells (outlined in red in Figure 4D, and **Figure S6B,C, S7B,D**). More apical regions of these glands typically contained strongly-staining K19⁺ cells, consistent with a surface epithelial phenotype (**Figure S6A, S7C**). Keratin 19 expression was especially strong in glands with squamous metaplasia (Fig. S6A, lower right). Infrequently, weakly-staining K19⁺ regions also contained expanded Dcamk11⁺ cells (outlined in black with arrowheads, and as magnified insets, Figure 4D, and arrowheads in Figure S7A, B). However, TFF2 and K19 expression were clearly distinct from Dcamk11, and colocalization of these markers was never observed in these serial sections or double immunofluorescence (Figure S7E). It appears that keratin 19 mRNA is expressed early on as the pit cell migrates upward through the gland, and prior to keratin 19 protein expression. Therefore, it is likely that K-ras is expressed in a few cells that are not reactive to the K19 antibody. While the transgene-derived mutant human K-ras could not be directly detected due to high homology with murine K-ras, we observed that K19 mRNA expression as assessed by in situ hybridization is present a few cells below keratin 19 protein⁺ cells, above the region where Dcamk11 is typically expressed (Figures S7F).

Similar immunohistochemical observations were made in regions of high-grade dysplasia, where Dcamk11⁺ cells were expanded but never coexpressed TFF2 or K19 (arrows in Figure 4D). Proliferating Ki67⁺ cells typically resided between the aforementioned cell types, although they were occasionally found to be TFF2⁺ (Figure 4D). Although we cannot completely exclude the possibility that the observed expansion of Dcamk11⁺ cells is due to expression of K-ras in these cells, the lack of colocalization with K19 mRNA and protein would suggest that it is more likely due to alterations in paracrine signals and/or their niche.

K19-kras transgenic mice display recruitment of BMDCs to the tumor microenvironment

To investigate the role of mutated K-ras in the recruitment of bone marrow derived cells (BMDCs) to the tumor microenvironment, we performed bone marrow transplantation (BMT) studies. Bone marrow from donor chicken beta actin-EGFP mice (WT/GFP) was transplanted into K19-kras or uninfected WT recipients. Six months after BMT, half of the bone marrow cells from recipient mice expressed GFP, similar to donor mice, with most of the GFP⁺ cells CD45⁺ hematopoietic cells (Figure S8A). Successful engraftment was confirmed by demonstration of GRP expression by mesenchymal stem cell cultures (Figure S8B), quantitative detection of transgene DNA sequences in BMT recipient bone marrow (Figure S8C), and detection of GFP⁺ cells in MSC cultures established from peripheral blood of all BMT recipient K19-kras mice (Figure S8B). Twelve to 18 months after BMT, gastric tissues

from K19-*kras* BMT recipient mice displayed all the phenotypic changes of non-transplanted K19-*kras* mice, including mucosal thickness, histological pathologies, shift of the Ki67⁺ proliferation zone, and dramatic expansion of Dcamk11⁺ cells (Figure S8B, D).

In the BMT recipient mice, only rare GFP⁺ cells were observed in the gastric mucosa of uninfected WT mice, while K19-*kras* mice had a greater than 10-fold increase in the number of recruited cells (Figure 5A-C). E-cadherin, an epithelial-specific cell surface molecule, was detected in all epithelial cells of the gastric epithelium, including dysplastic glands. More detailed analysis of the glandular areas with confocal microscopy revealed that, although a small number of GFP⁺ cells were E-cadherin(+) epithelial cells, a majority were E-cadherin (-) stromal cells (Figure 5D).

The expression of GFP was confirmed by immunohistochemically staining for GFP (Figure 5E). In addition, since GFP was present in only half of bone marrow cells (Figure S8A), we performed Y-chromosome in situ hybridization (Y-FISH) on sections prepared from female recipients that had received male donor bone marrow. Gastric sections showed many Y-chromosome⁺ cells in lymphoid follicles (Figure S8E) but no Y chromosome (+) cells in the gastric glands (Figure 5F). These findings suggest that the K19-expressing dysplastic gastric epithelium does not derive from the engrafted BMDCs.

To further characterize the GFP⁺ BMDCs, we performed immunofluorescent staining against CD45, vimentin, and alpha smooth muscle actin (α SMA). In all gastric sections, we detected colocalization of GFP with CD45, or spindle cells positive for vimentin, and/or α SMA, indicating the BMDCs had differentiated primarily into leukocytes, fibroblasts, and myofibroblasts, (Figure 6A). By 12 months, an estimated 15% of the recruited GFP⁺ BMDC in the gastric epithelium of WT mice with *H. felis* and K19*kras* mice were myofibroblasts, as characterized by their morphologic appearance and co-expression of α SMA (Figure S9).

To further understand the expansion of Dcamk11⁺ cells, we performed staining against GFP, α SMA and F4/80 in K19-*kras* BMT recipient mice. A plethora of GFP⁺ cells were found surrounding most clusters of Dcamk11⁺ cells. Excessive α -SMA⁺ stromal cells, as well as inflammatory F4/80⁺ macrophages, were typically seen surrounding these clusters, indicating that K-ras expression in adjacent putative progenitor cells favored an altered, inflammatory microenvironment (Figure 6B).

Discussion

In this study, we demonstrate that oncogenic K-Ras mutation in K19-expressing putative gastric epithelial progenitor cells activates inflammatory pathways and induces gastric atrophy, metaplasia, and dysplasia in a manner that largely parallels *H. felis*-induced carcinogenesis. K-ras-dependent chronic inflammation leads to recruitment of BMDCs that contribute primarily to the stromal microenvironment, and correlates with expansion of Dcamk11⁺ putative progenitor cells and development of high-grade dysplasia and rarely intramucosal carcinoma. Interestingly, *H. felis* infection of K19-Kras mice did not accelerate gastric cancer progression in these mice (data not shown), suggesting that the two models (K-ras mutation and *H. felis* infection) may progress through overlapping and/or non-additive pathways. Taken together, K-ras mutation is able to compensate for a lack of infectious stimulus, such as *H. felis* infection, to induce inflammation and carcinogenesis.

The development of dysplasia in the K19-*kras* mouse was not entirely surprising, given the known role of K-ras as an oncogene for the pancreas and other organs in the mouse (11,12, 27), and the fact that K-ras mutations have been reported rarely in gastric cancer (28,29). Although previous reports have noted only gastric hyperplasia and mucous metaplasia in K19-

kras mice up to 18 months of age (13), the current study is the first to examine the phenotype in a pure inbred (C57BL/6) background.

Previous studies by our group have modeled gastric cancer in mice using chronic *Helicobacter* infection or transgenic overexpression of cytokines that can drive gastric carcinogenesis independent of *Helicobacter* infection (4). Indeed, many cancers arise in the setting of chronic inflammation, which likely plays a role in both the initiation and promotion of tumors (30) and can lead to oncogenic mutations by inducing proliferation and increasing the mutation rate (31). However, cancers are also thought to arise in the absence of chronic inflammation through spontaneous or carcinogen-induced mutations in key oncogenes and tumor suppressor genes, with inflammation developing later on (32). In this latter model, transformed cells produce inflammatory mediators that attract tumor promoting inflammatory cells and set up cytokine networks. Accordingly, a number of studies have also shown that specific oncogenic mutations lead to a chronic inflammatory state (6,7).

Oncogenic Kras mutation in epithelial cells induces a number of molecular pathways that intrinsically regulate cellular processes such as proliferation, survival, and migration, that contribute to tumorigenesis (1,12,33). However, another consequence of oncogenic Ras signaling in carcinogenesis is the upregulation of cytokines and chemokines (9-11). Indeed, most of the cytokine/chemokines elevated in K19-kras mouse in this study have been reported to promote tumor development (4,10,34,35). The development of chronic inflammation in the stomachs of K19-kras transgenic mice was associated with significant increases in CXCL1, IL-1 β , and IL-6. It has previously been reported that oncogenic Ras mutations are able to induce the secretion of IL-6, which acts in a paracrine and autocrine fashion to promote tumor growth (34). K-ras has also been shown to upregulate the expression of IL-1 β in epithelial cells, propagating and enhancing inflammatory networks (36). The chemokine CXCL1 is overexpressed in human gastric cancers (37), and is a known critical downstream mediator of mutant Ras that recruits neutrophils (38), supports angiogenesis (39), regulates the microenvironment (35), and directly promotes tumorigenesis (39). Moreover, CXCL1 (also known as Gro1) is associated with other epithelial cancers such as hepatocellular carcinoma, even in the absence of overt neutrophil recruitment (40). The induction of dysplasia by K-ras correlated most tightly in our study with increased CXCL1, but further studies will be required to understand the role of CXCL1 in gastric cancer progression.

K-ras is known to induce COX-2 expression largely through upregulation of COX-2 mRNA stability (41), and the phenotype of K19-kras mice shows striking similarities to mice that overexpress COX-2-derived prostaglandins in K19⁺ cells (25); notably, both K19-kras mice and K19-C2mE mice exhibit expansion of mucous-producing cells and eventual gastric tumor development. While we were unable to detect increased COX-2 expression before the development of moderate dysplasia, it is interesting to speculate that it may have a role in phenotype development. Furthermore, we noted lymphoid aggregates in K19-kras mice similar to those found in *H. felis*-infected mice. While the antigen responsible for this adaptive immune response is unknown, it is possible that mutant Kras peptides may induce the antigenic response, as previously suggested (42,43) and contribute to phenotype development.

Additional inflammatory chemokines and growth factors, such as CXCL5, HB-EGF, and Amphiregulin, were expressed relatively specific to the K19-kras mice compared to *H. felis* dependent chronic gastritis. CXCL5 is an additional potent neutrophil chemoattractant (44), linked to connective tissue remodeling, and has been associated with gastric cancer progression independent of *Helicobacter* infection (45,46). Heparin-binding EGF-like growth factor (HB-EGF) is expressed by both myeloid cells (47) and gastric cancer cells (48), and has been shown to play a role in wound healing and carcinogenesis. Amphiregulin is also a member of the EGF family that is expressed by epithelial cells and fibroblasts (49) and induced in tumor cells with

Ras mutations (50). Given the link between these growth factors and EGF receptor signaling, it seems likely that they contribute to the glandular proliferation and metaplasia phenotype in the K19-*kras* mice.

One of the consequences of K-*ras*-induced chronic inflammation was the recruitment of BMDCs to the stromal microenvironment in gastric dysplasia. Many of the BMDCs in BMT recipient K19-*kras* mice were infiltrating immune cells, consistent with a previous observations of lymphocyte infiltration in the pancreatic periduct and gastric mucosa of K19-*kras* mice (13). However, BMDCs in the K19-*kras* mouse also comprised fibroblasts and myofibroblasts (also known as Cancer-Associated Fibroblasts, or CAFs) that expressed vimentin \pm α -SMA, that surrounded the base of the dysplastic gastric glands. Stromal myofibroblasts are believed to contribute to the stem cell niche in the gastrointestinal tract (51,52), but as yet the effects of depleting these stromal cell populations is unknown. Previous studies have reported that many CAFs present in tumors are likely to be bone marrow derived (53), and evidence for the importance of a bone marrow contribution to tumor stroma has previously been recognized (54). Thus, this is the first study to demonstrate that K-*ras* mutation on its own can lead to the recruitment of BM-derived CAFs. Few epithelial cells were bone marrow-derived, in contrast to earlier reports in the *H. felis* murine model (3).

Interestingly, in the K19-*kras* mouse stomach, there was a gradual expansion of Dcamk11⁺ cells that moved down to the base of the gastric glands and clustered in a region adjacent to BM-derived myofibroblastic niche cells, similar to that observed in the intestinal crypts of APC/Min mice (20). Dcamk11-expressing cells have been proposed as a candidate progenitor cell fraction in both the stomach and intestine (19,20), raising the possibility that K-*ras* overexpression in K19 cells may lead to an expansion of the gastric progenitor pool in the K19-*kras* mouse. It is probable that the expansion of Dcamk11⁺ cells was due to paracrine signals from stromal cells and/or adjacent K19⁺ putative progenitors, rather than a direct effect of K-*ras* within Dcamk11⁺ cells, given that K19 and Dcamk11 were differentially expressed in most dysplastic cells. However, to date the only reported marker to lineage trace an entire gastric gland is Lgr5 (25). Since LGr5 lineage tracing is restricted to the antrum and dysplasia in K19-*kras* mice is found in the corpus, it is unlikely that Lgr5-derived cells are the primary source of the corpus dysplasia. However, definitive data as to the source of dysplastic lesions will require additional lineage tracing studies.

In conclusion, K-*ras* mutation in K19⁺ putative gastric tissue progenitor cells induced pro-inflammatory responses, resulting in early onset of gastric dysplasia. Dcamk11⁺ cells were found clustered in dysplastic glands, adjacent to expanded K19⁺ regions. BMDCs contributed significantly to the microenvironment of dysplastic glands as immune cells, fibroblasts, and myofibroblasts. Further characterization of the relationship between K19⁺ and Dcamk11⁺ cells in the normal gastric epithelium and dysplastic lesions may provide greater insight into the cellular and molecular mechanisms of carcinogenesis.

Supplementary Material

Refer to Web version on PubMed Central for supplementary material.

Acknowledgments

The authors wish to thank Dr. Melitta Penz, and Ms. Shanisha Gordon for animal care and technical assistances.

This work was supported by grants 5R01 CA120979-02 (TCW), R01 DK060694 (AKR) U01 CA143056 (TCW, AKR) and P30 DK050306 (Mouse Core) from the NIH and The Uehara Memorial Foundation.

References

1. Milne AN, Carneiro F, O'Morain C, Offerhaus GJ. Nature meets nurture: molecular genetics of gastric cancer. *Hum Genet* 2009;126:615–28. [PubMed: 19657673]
2. Chan AO, Chu KM, Huang C, et al. Association between *Helicobacter pylori* infection and interleukin 1beta polymorphism predispose to CpG island methylation in gastric cancer. *Gut* 2007;56:595–7. [PubMed: 17369391]
3. Houghton J, Stoicov C, Nomura S, et al. Gastric cancer originating from bone marrow-derived cells. *Science* 2004;306:1568–71. [PubMed: 15567866]
4. Tu S, Bhagat G, Cui G, et al. Overexpression of interleukin-1beta induces gastric inflammation and cancer and mobilizes myeloid-derived suppressor cells in mice. *Cancer Cell* 2008;14:408–19. [PubMed: 18977329]
5. Oguma K, Oshima H, Aoki M, et al. Activated macrophages promote Wnt signaling through tumor necrosis factor-alpha in gastric tumor cells. *EMBO J* 2008;27:1671–81. [PubMed: 18511911]
6. Lin WW, Karin M. A cytokine-mediated link between innate immunity, inflammation, and cancer. *J Clinical Invest* 2007;117:1175–83. [PubMed: 17476347]
7. Andreu P, Johansson M, Affara NI, et al. FcRgamma activation regulates inflammation-associated squamous carcinogenesis. *Cancer Cell* 2010;17:121–34. [PubMed: 20138013]
8. Frame S, Balmain A. Integration of positive and negative growth signals during Ras pathway activation in vivo. *Curr Opin Genet Dev* 2000;10:106–13. [PubMed: 10679397]
9. Abrams SI, Stanziale SF, Lunin SD, Zaremba S, Schlom J. Identification of overlapping epitopes in mutant ras oncogene peptides that activate CD4+ and CD8+ T cell responses. *Eur J Immunol* 1996;26:435–43. [PubMed: 8617315]
10. Sparmann A, Bar-Sagi D. Ras-induced interleukin-8 expression plays a critical role in tumor growth and angiogenesis. *Cancer Cell* 2004;6:447–58. [PubMed: 15542429]
11. Ji H, Houghton AM, Mariani TJ, et al. K-ras activation generates an inflammatory response in lung tumors. *Oncogene* 2006;25:2105–12. [PubMed: 16288213]
12. Hingorani SR, Petricoin EF, Maitra A, et al. Preinvasive and invasive ductal pancreatic cancer and its early detection in the mouse. *Cancer Cell* 2003;4:437–50. [PubMed: 14706336]
13. Brembeck FH, Schreiber FS, Deramaudt TB, et al. The mutant K-ras oncogene causes pancreatic periductal lymphocytic infiltration and gastric mucous neck cell hyperplasia in transgenic mice. *Cancer Res* 2003;63:2005–9. [PubMed: 12727809]
14. Sparmann A, Bar-Sagi D. Ras oncogene and inflammation: partners in crime. *Cell Cycle* 2005;4:735–6. [PubMed: 15908805]
15. Borrello MG, Degl'Innocenti D, Pierotti MA. Inflammation and cancer: the oncogene-driven connection. *Cancer Letters* 2008;267:262–270. [PubMed: 18502035]
16. Brembeck FH, Moffett J, Wang TC, Rustgi AK. The keratin 19 promoter is potent for cell-specific targeting of genes in transgenic mice. *Gastroenterology* 2001;120:1720–8. [PubMed: 11375953]
17. Calnek D, Quaroni A. Changes in keratin expression during fetal and postnatal development of intestinal epithelial cells. *Biochem J* 1992;285:939–46. [PubMed: 1379798]
18. Calnek D, Quaroni A. Differential localization by in situ hybridization of distinct keratin mRNA species during intestinal epithelial cell development and differentiation. *Differentiation* 1993;53:95–104. [PubMed: 7689500]
19. Giannakis M, Stappenbeck TS, Mills JC, et al. Molecular properties of adult mouse gastric and intestinal epithelial progenitors in their niches. *J Biol Chem* 2006;281:11292–300. [PubMed: 16464855]
20. May R, Riehl TE, Hunt C, Sureban SM, Anant S, Houchen CW. Identification of a novel putative gastrointestinal stem cell and adenoma stem cell marker, doublecortin and CaM kinase-like-1, following radiation injury and in adenomatous polyposis coli/multiple intestinal neoplasia mice. *Stem Cells* 2008;26:630–7. [PubMed: 18055444]
21. Rogers AB, Taylor NS, Whary MT, Stefanich ED, Wang TC, Fox JG. *Helicobacter pylori* but not high salt induces gastric intraepithelial neoplasia in B6129 mice. *Cancer Res* 2005;65:10709–15. [PubMed: 16322215]

22. Rogers AB, Houghton J. Helicobacter-based mouse models of digestive system carcinogenesis. *Methods Mol Biol* 2009;511:267–95. [PubMed: 19347301]
23. Wang SS, Asfaha S, Okumura T. Fibroblastic colony-forming unit bone marrow cells delay progression to gastric dysplasia in a helicobacter model of gastric carcinogenesis. *Stem Cells* 2009;27:2301–11. et. al. [PubMed: 19591219]
24. Rosselot C, Spraggon L, Chia I, et al. Non-cell autonomous retinoid signaling is crucial for renal development. *Development* 2010;137:283–292. [PubMed: 20040494]
25. Oshima H, Oshima M, Inaba K, Taketo MM. Hyperplastic gastric tumors induced by activated macrophages in COX-2/mPGES-1 transgenic mice. *EMBO J* 2004;23:1669–1678. [PubMed: 15014433]
26. Barker N, Huch M, et al. Lgr5+ve Stem Cells Drive Self-Renewal in the Stomach and Build Long-Lived Gastric Units In Vitro. *Cell Stem Cell* 2010;6:25–36. [PubMed: 20085740]
27. Habbe N, Shi G, Meguid RA, et al. Spontaneous induction of murine pancreatic intraepithelial neoplasia (mPanIN) by acinar cell targeting of oncogenic Kras in adult mice. *PNAS* 2008;105:18913–8. [PubMed: 19028870]
28. Watari J, Tanaka A, Tanabe H, et al. K-ras mutations and cell kinetics in Helicobacter pylori associated gastric intestinal metaplasia: a comparison before and after eradication in patients with chronic gastritis and gastric cancer. *J Clin Pathol* 2007;60:921–6. [PubMed: 16997920]
29. Hiyama T, Haruma K, Kitadai Y, et al. K-ras mutation in helicobacter pylori-associated chronic gastritis in patients with and without gastric cancer. *Int J Cancer* 2002;97:562–6. [PubMed: 11807778]
30. de Visser KE, Eichten A, Coussens LM. Paradoxical roles of the immune system during cancer development. *Nat Rev Cancer* 2006;6:24–37. [PubMed: 16397525]
31. Fox JG, Wang TC. Inflammation, atrophy, and gastric cancer. *J Clin Invest* 2007;117:60–9. [PubMed: 17200707]
32. Balkwill F, Charles KA, Mantovani A. Smoldering and polarized inflammation in the initiation and promotion of malignant disease. *Cancer Cell* 7:211–7. 200. Review. [PubMed: 15766659]
33. Schubert S, Shannon K, Bollag G. Hyperactive Ras in developmental disorders and cancer. *Nat Rev Cancer* 2007;7:295–308. Review. [PubMed: 17384584]
34. Ancrile B, Lim KH, Counter CM. Oncogenic Ras-induced secretion of IL6 is required for tumorigenesis. *Genes Dev* 2007;21:1714–9. [PubMed: 17639077]
35. Yang G, Rosen DG, Zhang Z, et al. The chemokine growth-regulated oncogene 1 (Gro-1) links RAS signaling to the senescence of stromal fibroblasts and ovarian tumorigenesis. *PNAS* 2006;103:16472–7. [PubMed: 17060621]
36. Takahashi M, Mutoh M, Shoji Y, et al. Transfection of K-rasAsp12 cDNA markedly elevates IL-1beta- and lipopolysaccharide-mediated inducible nitric oxide synthase expression in rat intestinal epithelial cells. *Oncogene* 2003;22:7667–76. [PubMed: 14576830]
37. Junnila S, Kokkola A, Mizuguchi T, et al. Gene expression analysis identifies over-expression of CXCL1, SPARC, SPP1, and SULF1 in gastric cancer. *Genes Chromosomes Cancer* 2010;49:28–39. [PubMed: 19780053]
38. Moser B, Clark-Lewis I, Zwahlen R, Baggiolini M. Neutrophil-activating properties of the melanoma growth-stimulatory activity. *J Exp Med* 1990;171:1797–1802. [PubMed: 2185333]
39. Haghnegahdar H, Du J, Wang D, et al. The tumorigenic and angiogenic effects of MGSA/GRO proteins in melanoma. *J Leukoc Biol* 2000;67:53–62. [PubMed: 10647998]
40. Fox JG, Feng Y, et al. Gut microbes define liver cancer risk in mice exposed to chemical and viral transgenic hepatocarcinogens. *Gut* 2010;59:88–97. [PubMed: 19850960]
41. Zhang Z, Sheng H, et al. Posttranscriptional regulation of cylooxygenase-2 in rat intestinal epithelial cells. *Neoplasia* 2000;2:523–30. [PubMed: 11228545]
42. Shono Y, Tanimura H, et al. Specific T-cell immunity against Ki-ras peptides in patients with pancreatic and colorectal cancers. *Br. J. Cancer* 2003;88:530–536. [PubMed: 12592366]
43. Bristol JA, Orsini C, Lindinger P, Thalhamer J, Abrams SI. Identification of a ras oncogene peptide that contains both CD4+ and CD8+ T cell epitopes in a nested configuration and elicits both T cell subset responses by peptide or DNA immunization. *Cell Immunol* 2000;205:73–83. [PubMed: 11104579]

44. Qiu Y, Zhu J, Bandi V, et al. Biopsy neutrophilia, neutrophil chemokine and receptor gene expression in severe exacerbations of chronic obstructive pulmonary disease. *Am J Respir Crit Care Med* 2003;168:968–75. [PubMed: 12857718]
45. Park JY, Park KH, Bang S, et al. CXCL5 overexpression is associated with late stage gastric cancer. *J Cancer Res Clin Oncol* 2007;133:835–40. [PubMed: 17479287]
46. Sieveking D, Mitchell HM, Day AS. Gastric epithelial cell CXC chemokine secretion following *Helicobacter pylori* infection in vitro. *J Gastroenterol Hepatol* 2004;19:982–7. [PubMed: 15304113]
47. Besner G, Higashiyama S, Klagsbrun M. Isolation and characterization of a macrophage-derived heparin binding growth factor. *Cell Regul* 1990;1:811–9. [PubMed: 2088527]
48. Dickson JH, Grabowska A, El-Zaatari M, Atherton J, Watson SA. *Helicobacter pylori* can induce heparin-binding epidermal growth factor expression via gastrin and its receptor. *Cancer Res* 2006;66:7524–31. [PubMed: 16885350]
49. Shoyab M, Plowman GD, McDonald VL, Bradley JG, Todaro GJ. Structure and function of human amphiregulin: a member of the epidermal growth factor family. *Science* 1989;243:1074–6. [PubMed: 2466334]
50. Toulany M, Dittmann K, Krüger M, Baumann M, Rodemann HP. Radioresistance of K-Ras mutated human tumor cells is mediated through EGFR-dependent activation of PI3K-AKT pathway. *Radiother Oncol* 2005;76:143–50. [PubMed: 16024124]
51. Direkze NC, Hovalva-Dilke K, Jeffery R, et al. Bone marrow contribution to tumor-associated myofibroblasts and fibroblasts. *Cancer Res* 2004;64:8492–5. [PubMed: 15574751]
52. Studeny M, Marini FC, Dembinski JL, et al. Mesenchymal stem cells: potential precursors for tumor stroma and targeted-delivery vehicles for anticancer agents. *J Natl Cancer Inst* 2004;96:1593–603. [PubMed: 15523088]
53. Ishii G, Sangai T, Oda T, et al. Bone-marrow-derived myofibroblasts contribute to the cancer-induced stromal reaction. *Biochem Biophys Res Commun* 2003;309:232–240. [PubMed: 12943687]
54. Guo X, Oshima H, Kitmura T, et al. Stromal Fibroblasts Activated by Tumor Cells Promote Angiogenesis in Mouse Gastric Cancer. *J Biol Chem* 2008;283:19864–71. [PubMed: 18495668]

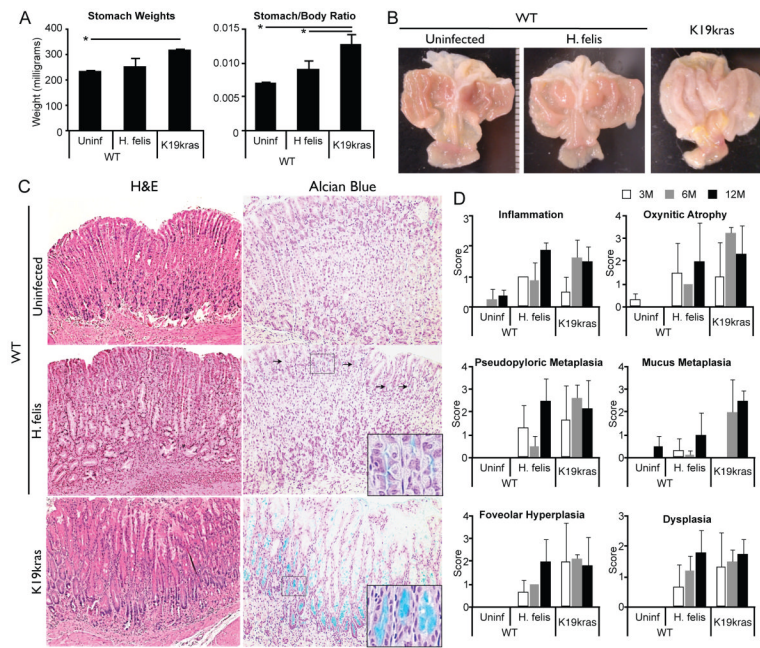


Figure 1. Gastric histology of WT and K19-kras mice

A-C. From mice 12 month cohort: body and stomach weights (A), representative gross presentation (B), and H&E- and alcian blue-stained gastric tissue sections (C). Representative Alcian blue⁺ cells in WT *H. felis* infected mice indicated by arrows, magnified insets are of boxed regions (original magnification 100 and 150x, respectively). D. Histopathology scores for gastric lesions of the mice at 3, 6, 12 months after *H. felis* infection (* $p < 0.01$, $n = 3$ for each group).

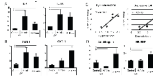


Figure 2. Expression of chemokines/cytokines/growth factors

A, B, D. Quantitative real-time RT-PCR analysis of 12 month cohort (*p<0.1, §p<0.05, n>3 in each group)

C. Relationship between dysplasia score and mRNA expression of CXCL1 and IL-6 in K19-kras mice at 12 months.

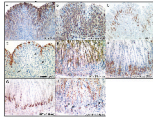


Figure 3. Immunohistochemical staining in gastric epithelium of uninfected wild type and K19-kras mice at 12 months

Expression of K19 (A, E), H/K ATPase (B, F), Ki67 (C, G), and Dcamk11 (D, H) in the gastric epithelium of WT (A-D) and K19-kras (E-H) mice (arrows indicate Dcamk11⁺ cells, original magnification 150x).

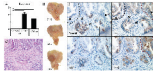


Figure 4. Aged K19-kras mice develop high-grade dysplasia

- A. Histopathology scores for dysplasia in gastric lesions of mice between 16 and 19 months
- B. Gross presentation of the stomachs with papillary tumors. Stomachs from a WT mouse 19 months with *H. felis* infection (7445) and K19-kras mice at 16 to 19 months (9003 and 7456, respectively).
- C. H&E-stained gastric tissue section of a K19-kras mouse at 16 months displaying submucosal penetration of intramucosal carcinoma (original magnification 200x)
- D. Expression of Dcamk11, K19, Ki67, and TFF2 in low- and high-grade dysplasia of a K19-kras mouse (original magnification 300x).

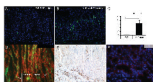


Figure 5. Detection of BMDCs in the gastric epithelium of recipient mice

Endogenous GFP fluorescence of BMDCs in gastric tissue of WT (A) or K19-kras (B) BMT recipients (original magnification, 150x), quantified in (C) (* $p < 0.01$, $n = 3$ per group).

D. Representative E-cadherin (red) and GFP (green) in gastric tissue of K19-kras BMT recipients. (original magnification, 200x). Magnified inset of a representative double positive cell (bone marrow-derived epithelial cell) and GFP single positive cells (bone marrow-derived stromal cells) are shown.

E. Representative immunohistochemistry for GFP in K19-kras BMT recipients detected by (original magnification, 200x).

F. Y-FISH (red) in a gastric tissue section of a K19-kras female receiving male donor BMT (original magnification, 400x).

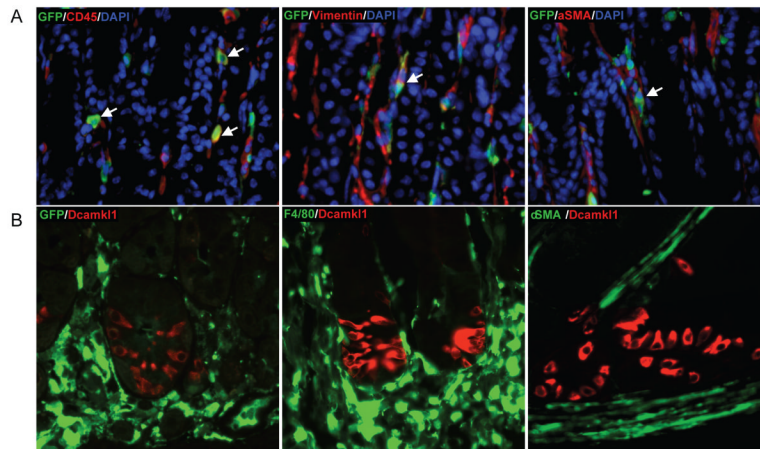


Figure 6. Characterization of BMDCs in BMT recipient mice

Gastric tissue sections from K19-kras BMT recipients detecting (A) endogenous GFP of BMDCs, and stained red for CD45 (left), vimentin (middle), and (B) α SMA (right), and endogenous GFP (left, from a BMT recipient), or stained for F4/80 (middle, green) or α SMA (right, green) and stained for Dcamk11 (red, original magnification, 400x)